



Supramolecular assembly of hydrophilic Co(III)-porphyrin with bidentate ligands in aqueous buffer media



Galina M. Mamardashvili, Elena Yu. Kaigorodova, Ivan S. Lebedev, Il'ya A. Khodov,
Nugzar Z. Mamardashvili*

G.A. Krestov Institute of Solution Chemistry of the Russian Academy of Sciences, Akademicheskaya st.1, 153045 Ivanovo, Russia

ARTICLE INFO

Keywords:
Non-covalent interactions
Self-assembly
Supramolecular arrays
Porphyrin
Micelles

ABSTRACT

The processes of hydrophilic Co(III)-tetra(4-sulfonatophenyl)porphyrin supramolecular assembly with 4,4-bipyridyl in aqueous buffer media have been studied by UV-vis, 1D and 2D ^1H NMR-spectroscopy. In the case of 1,4-diazabicyclo[2.2.2]octane, pyrazine and piperazine in aqueous solutions, no assembly was observed. Interactions of the hydrophilic Co(III)-tetraarylporphyrin with ionic micelles (cationic surfactants with different alkyl tail lengths) in buffer media were investigated. These studies were performed by the UV-vis, ^1D NOESY-spectroscopy and dynamic lightscattering (DLS) methods. The metalloporphyrins were incorporated into the hydrophobic part of micelles, which led to Co(III) reduction to Co(II) in the Co-porphyrinate composition. The rate of Co(III) reduction accompanied by detachment of additional ligands coordinated on Co(III)-porphyrins or disruption of supramolecular dimers and depends on the surfactant concentration and nature. The results obtained indicate the possibility of creating of supramolecular porphyrin-based assemblies with the preprogrammed lifetime (from several hours to several days) and could be used in the creation of host-guest systems for recognition, selective binding and prolonged release of bioactive substrates as the means in the designing of biomimetic systems with effective binding affinities to heterocycles, DNA base pairs and RNA.

1. Introduction

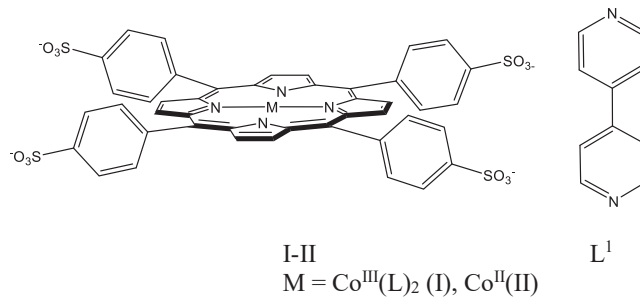
Supramolecular chemistry is one of the most popular and rapidly developing fields of experimental chemistry. The latest advances in supramolecular chemistry and the most promising fields of its practical application are related to the processes of molecular recognition and formation of new, spatially pre-organized structures due to the so-called “self-processes” - self-assembly and self-organization [1,2]. Porphyrin molecules are quite common in nature and porphyrin supramolecular assemblies are widely used as models for photosynthesis processes studying [3,4]. Of great interest is a novel development in the field of binding affinities of self-assembled metal porphyrins to heterocycles, DNA base pairs and RNA [5]. Supramolecular oligomeric porphyrins and metalloporphyrins with various structures are also intensively studied as potential molecular wires, molecular switches, photonic tubes and molecular elements for storing information [6,7]. However, it should be noted that most of the porphyrin supramolecular assemblies described so far in the literature have been obtained from lipophilic tetrapyrrole macrocycles in non-aqueous solvents [8–23]. Self-assembly

and self-organization of porphyrin and metalloporphyrin molecules in aqueous media have received much less attention. Moreover, in case of hydrophilic macrocycles, they have their own specific features. In aqueous media, these processes have their own regularities, and self-assembly can be additionally controlled by changing the medium pH and surfactant additives leading to micellization of porphyrin molecules and supramolecular complexes based on them. The aim of this work is to study the processes of molecular recognition and supramolecular assembly of hydrophilic Co(III)-porphyrin with bidentate ligands in aqueous buffer media and conditions for decomposition of metalloporphyrin arrays due to the Co(III) reduction to Co(II). The reduction of Co(III) to Co(II) in sulfonated Co-porphyrins occurs upon their incorporation into spherical micelles of cationic surfactants of different nature. Depending on the lengths of the alkyl tail surfactants and their concentration, it is possible to produce porphyrin arrays with a pre-programmed life time. The porphyrin dimers with bipyridyl described in this work are the simplest hydrophilic supramolecular assemblies with the participation of Co-porphyrins. They are of interest as building blocks for multi-porphyrin arrays with noncovalent interactions in

* Corresponding author.

E-mail address: ngm@isc-ras.ru (N.Z. Mamardashvili).

aqueous solutions. Such species are promising for designing photoactive molecular devices and as models for solar energy harvesting and biomimetic systems.



2. Experimental

2.1. Materials

Bidentate ligand: 4,4'-dipyridyl (L¹), pyrazine (L²), piperazine (L³) and 1,4-diazabicyclo[2.2.2]octane (DABCO, L⁴), 5,10,15,20-tetra-(4-sulfophenyl)porphyrin sodium salt, cetyltrimethylammonium bromide (CTAB) and myristyltrimethylammonium bromide(MTAB) reagents were produced by Sigma-Aldrich.

Bis-aqua-Co(III)-tetra(4-sulfophenyl)porphyrin [CoP(OH₂)₂] (I) was synthesized by the procedure described in [24] by boiling *meso*-tetra(4-sulfophenyl)porphyrin with CoCl₂ in DMFA. Yield: 25.1 mg (96 %). UV-Vis (phosphate pH 7.4 buffer) λ_{max} , nm (lge): 426.0 (5.01), 542.0 (3.96); ¹H NMR(500 MHz, D₂O) δ, ppm: 9.14 (s, 8H, β-Porph.), 8.31 (d, 8H, J = 7.8, *ortho*-Ph), 8.12 (d, 8H, J = 7.8 *meta*-Ph); Calculated, %: C 48.94; H 2.24; N 5.19. C₄₄H₂₄CoN₄S₄O₁₂Na₄. Found, %: C 48.91; H 2.22; N 5.16; Mass spectrum: *m/z* (*I_{rel}*, %) (M = C₄₄H₂₄CoN₄S₄O₁₂): 986 (100) [M]⁻, 1004 (28) [M + H₂O]⁻, 1023 (11) [M + 2(H₂O)]⁻.

2.1.1. Co(III)P(L¹)(H₂O) (I-L¹)

UV-Vis (phosphate buffer pH 7.4) λ_{max} , nm (lge): 428.3 (4.86), 545.3 (3.90). ¹H NMR (500 MHz, D₂O) δ, ppm: 9.12 (s, 8H, β-Por.), 8.18 (d, 8H, J = 7.6, *ortho*-Ph), 7.92 (d, 8H, J = 7.2, *meta*-Ph), 8.52 (d, 2H, J = 4.2, H⁰(L), 7.65 (d, 2H, J = 7.2, H^m(L), 6.49 (d, 4H, J = 7.2, H^m(L), 2.22 (d, 4H, J = 4.2, H⁰(L); Mass spectrum: *m/z* (*I_{rel}*, %) (M = C₄₄H₂₄CoN₄S₄O₁₂): 986 (100) [M]⁻, 1004 (19) [M + H₂O]⁻, 1142 (31) [(M + L¹]⁻].

2.1.2. Co(III)P(L¹)₂ (L¹-I-L¹)

UV-Vis (phosphate buffer pH 7.4) λ_{max} , nm (lge): 429.7 (4.86), 549.3 (3.90). ¹H NMR (500 MHz, D₂O) δ, ppm: 9.12 (bs, s, 8H, β-Por.), 8.11 (d, J = 7.6, 8H, *ortho*-Ph), 7.96 (d, J = 7.8, 8H, *meta*-Ph), 8.49 (d, 4H, J = 4.2, H⁰(L), 7.62 (d, 4H, J = 7.2, H^m(L), 6.40 (d, J = 7.2, 4H, H^m(L), 2.28 (d, 4H, J = 7.2, H⁰(L); Mass spectrum: *m/z* (*I_{rel}*, %) (M = C₄₄H₂₄CoN₄S₄O₁₂): 986(100) [M]⁻, 1142 (19) [(M + L¹]⁻, 1298 (10) [(M + 2L¹]⁻].

2.1.3. Co(III)P(L¹)Co(III)P (I-L¹-I)

UV-Vis (phosphate buffer pH 7.4) λ_{max} , nm (lge): 428.8 (4.88), 545.5 (3.92). ¹H NMR (500 MHz (D₂O)) δ, ppm: 9.10 (s, 16H, H^β(I)), 7.86 (d, 16H, J = 7.6, H⁰(I)), 7.71 (d, 16H, J = 7.8, H^m(I)), 5.85 (d, J = 7.4, 4H, H^m(L), 1.78 (d, 4H, J = 4.4, H⁰(L). Mass spectrum: *m/z* (*I_{rel}*, %) (M = C₄₄H₂₄CoN₄S₄O₁₂): 986(100) [M]⁻, 1142 (31) [M + L¹]⁻, 2128 (11) [M + L¹ + M]⁻ (Fig. S1).

3. Methods and measurements

3.1. Spectrophotometric studies

UV-vis spectra were recorded at room temperature in an air-tight optical cell (10 mm) on a Jasco V-770 spectrophotometer. The thermodynamic constants for the complexation of MP with L were calculated according to the Equation based on the spectrophotometric titration experiment results:

$$K = \frac{[MP - L]}{[MP][L]} = \frac{1}{[L]} \left(\frac{\Delta A_{i, \lambda_1}}{\Delta A_{o, \lambda_1}} \times \frac{\Delta A_{o, \lambda_2}}{\Delta A_{i, \lambda_2}} \right), \quad M^{-1}$$

where λ_1 is the descending wavelength, λ_2 is the ascending wavelength; [MP-L] is the concentration of the porphyrinate with one axial ligand; and [L] is the ligand concentration. ΔA_0 is the maximal change in the solution optical density at the given wavelength, and ΔA_i is the change in the solution optical density at the given wavelength at the given concentration [25].

The thermodynamic constants for the complexation of the MP-L-MP dimer were calculated.

$$K = \frac{[MP - L - MP]}{[MP]^2[L]} = \frac{1}{[L][MP]} \left(\frac{\Delta A_{i, \lambda_1}}{\Delta A_{o, \lambda_1}} \times \frac{\Delta A_{o, \lambda_2}}{\Delta A_{i, \lambda_2}} \right), \quad M^{-2}$$

The kinetic parameters of the investigated reaction were obtained according to the known procedure [26]. The effective rate constants (k_{eff}) were determined by the change in the solution optical density at working wave lengths ($\lambda = 414, 425$ nm) after definite time intervals with a CTAB excess.

$$k_{\text{eff}} = \frac{1}{\tau} \lg \frac{C_0}{C_\tau}$$

where C_0 and C_τ are the concentrations of the complexes at the onset of the process and at a time τ . The k_{eff} values were determined by the Guggenheim method [27]. The relative error was 3–5%.

3.1.1. NMR studies

The selective ¹D NOESY experiment [28–30] was carried out using selective refocusing with a shaped pulse with the mixing time duration of 0.8 s. Selective Gaussian pulse of 80 ms was used to refocus the resonance. The NMR experiments were performed on a BrukerAvance III500 MHz NMR spectrometer (BrukerBiospin, Karlsruhe, Baden-Württemberg, Germany) equipped with a 5-mm probe using standard Bruker TOPSPIN Software. The temperature was controlled using a Bruker variable temperature unit (BVT-2000) in combination with a Bruker cooling unit (BCU-05) to provide chilled air. The experiments were performed at 298 K without sample spinning. TMS signals were used as internal standards to count the chemical shifts. The two-dimension diffusion ordered spectroscopy (2D DOSY) spectra were recorded with a PGSTE pulse sequence using bipolar gradient pulses and a supplementary delay (LED) insertion [31]. The PGSTE sequence was used with a diffusion delay of 0.1 s, with the total diffusion-encoding pulse width of 5 ms. For each of the 32 gradient amplitudes, 32 transients of 16,384 complex data points were obtained. 2D COSY spectra with a zero-quantum suppression element [32] were recorded with a 16.96 ppm spectral window in the direct F1 dimension with 2048 complex data points and a 16.96 ppm spectral window in the indirect F2 dimension with 128 complex points. The spectra were obtained with 64 scans and relaxation delay of 2 s. The two-dimensional rotating frame nuclear Overhauser effect spectroscopy (2DROESY) [32] experiments were performed by pulsed filtered gradient techniques. The spectra were recorded in a phase sensitive mode using Echo/Antiecho-TPPI gradient selection with 2048 points in the F2 direction and 256 points in the F1 direction.

The pH was monitored by an Electroanalytical Analyser (Type OP-300, Radelkis)ion meter. Micelle sizes were measured by dynamic

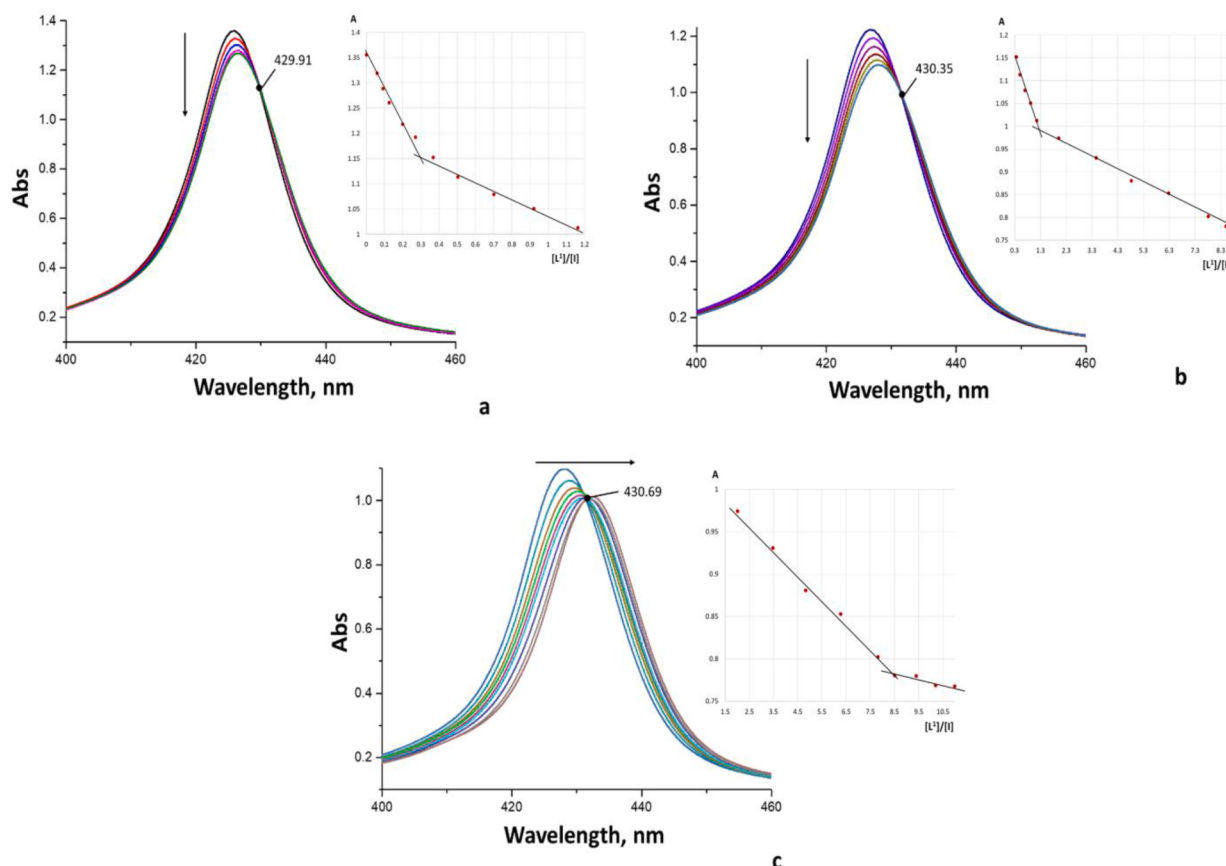
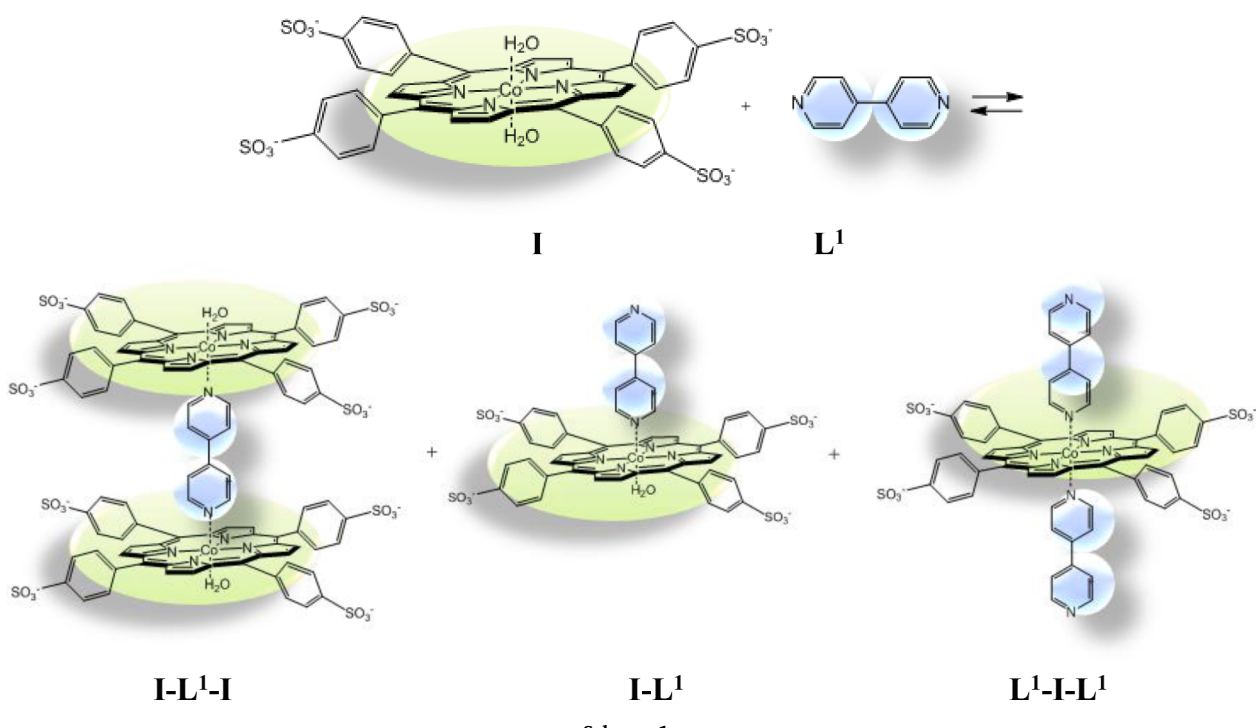


Fig. 1. UV-vis spectra (Soret band region) of the Co(III)P phosphate buffer solution ($\text{pH} = 7.4$) upon titration with L1 with three groups of isobestic points: (a) the first group of spectral curves ($C_{\text{L}} = 0 - 4 \times 10^{-6} \text{ M}$); (b) the second group of spectral curves ($C_{\text{L}} = 4.1 \times 10^{-6} - 2.0 \times 10^{-5} \text{ M}$); (c) the third group of spectral curves ($C_{\text{L}} = 2.2 \times 10^{-5} - 1.1 \times 10^{-4} \text{ M}$) ($C_{\text{porph.}} = 8.0 \times 10^{-6}$, 25°C).



Scheme 1.

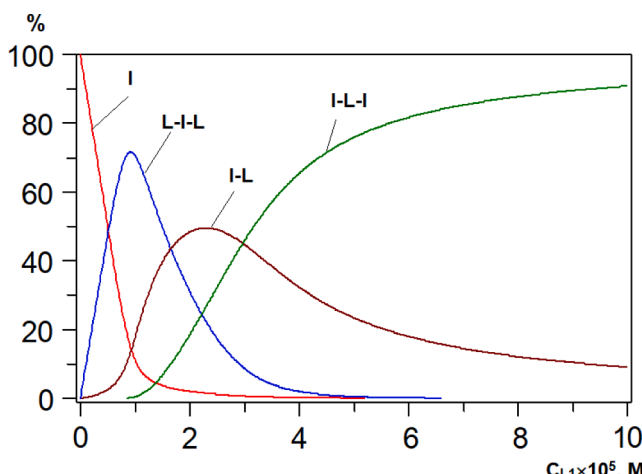


Fig. 2. Distribution of particles by mole fractions of complexes I-L¹-I, I-L¹ and L¹-I-L¹ depending on the L¹ concentration (C_I = const).

light scattering on a Zetasizer Nano ZS instrument, Malvern Instruments.

3.2. Mass spectrometry

The mass spectra were obtained on a Brukermicro TOF mass spectrometer (in H₂O as the solvent). High-resolution spectra were recorded on a Bruker maXis time-of-flight mass spectrometer with electrospray ionization (ESI-MS).

4. Results and discussion

4.1. Investigation of the Co(III)-porphyrin interaction with bidentate ligands in buffer media

The processes of supramolecular self-assembly of various metalloporphyrin assemblies based on various polydentate ligands in organic solvents (dichloromethane, toluene, benzene) are described in [9–14]. In most cases, the building blocks for the preparation of supramolecular porphyrin assemblies are zinc porphyrinates. Our studies have shown that the self-assembly processes of porphyrinates in organic and aqueous media differ from each considerably. While in organic solvents of two metalporphyrinates (Zn- and Co-), the most stable supramolecular arrays are formed on the basis (with the participation) of zinc-porphyrins, the opposite is observed in aqueous media. In aqueous media, hydrophilic cobalt porphyrinates are in the form of bis-aquacomplexes (I), in which water molecules can be replaced by various organic bases. Substitution proceeds sequentially with the formation of mono-axial and biaxial complexes [33–35]. In the interaction of cobalt-porphyrins with bidentate ligands, the formation of a third type of products, supramolecular dimers, is theoretically possible; however, in practice, dimers are rarely formed. The study of the interaction of I with a number of bidentate ligands (L¹-L⁴) showed that the products of this interaction depend on the nature of the ligand. Porphyrinate I with L⁴ (DABCO) forms only one complex type – a binary complex (I-L) with a very low stability constant. The products of interaction of I with bidentate ligands L² and L³ are two complex types – I-L and L-I-L. The titration curves of complex I with these ligands show two stages, each corresponding to its own group of isobestic points on the spectral curves (Fig. 1). The titration curve of complex I with L¹ has three stages with respective isobestic point groups, which indicates the formation of three complex types: I-L¹-I, I-L¹ and L¹-I-L¹ (Fig. 1), according to equations (1–5) that are derived from scheme 1.

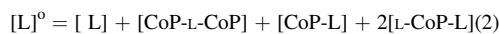


Table 1
Stability constants of the Co(III)P complexes with L.

Complex composition	(H ₂ O)Co(III)P-L-Co(III) P(H ₂ O) [2CoP + L], M ⁻²	Co(III)(L)(H ₂ O) [CoP + L], M ⁻¹	Co(III)(L) ₂ [CoP(L) + L], M ⁻¹
L ¹	1.5×10^{10}	5.1×10^4	3.2×10^3
L ²	–	1.2×10^4	5.7×10^2
L ³	–	3.5×10^3	1.9×10^2
L ⁴	–	1.9×10^2	–

$$K_{21} = [CoP-L-CoP]/[CoP]²[L](3)$$

$$K_{11} = [CoP-L]/[CoP][L](4)$$

$$K_{12} = [L-CoP-L]/[CoP-L][L](5)$$

Fig. 2 shows the concentration profiles obtained by adjusting the whole series of spectra to the model shown in Scheme 1 using Hyperquad Simulation and Speciation [36]. The mole fraction of the I-L¹-I reaches a maximum of 72% after adding 0.8 L¹ equivalents and decreases to 10% when 3 L¹ equivalents are used. The maximum amount of binary I-L¹ complexes is 49% when 1.5 L¹ equivalents are added. After adding 4 equivalents of L¹, porphyrinate I is predominantly found in the form of diaxial complexes - L¹-I-L¹.

The stability constants of the complexes obtained by spectrophotometric titration are presented in Table 1. The pH value of the buffer medium in the range of 4.0–9.0 has no significant effect on the aforementioned processes (Table S1). The UV-vis spectra of the obtained complexes of I with L¹ are shown in Table S2.

The I-L¹-I complex is supramolecular. The difference between self-assembly and simple coordination is that self-assembly processes involve multiple interactions including one or more closed loops. At the same time, coordination to one site of a multi-dentate ligand can affect the affinity of the other sites (through steric, conformational, or electrostatic communication). The ¹H NMR-spectra of I and its L¹-L, I-L¹ and L¹-I-L¹ complexes are presented in Fig. 3, Tables 2 and S3.

The signals in the ¹H NMR spectra were assigned by conducting 2D NMR-COSY experiments. Fig. 3 shows the (¹H-¹H) COSY spectrum of the solution of compound I with 0.5 L¹ equivalents as an example. The spectrum contains cross-peaks between the phenyl-group proton signals of the tetrapyrrole fragments and axial dipyridyl ligand located between these porphyrinates. In addition to the main signals of the dimer, the spectrum shows cross peaks between the phenyl group proton signals of the monomer porphyrinates and non-bound bidentate ligand. An analysis of the DOSY spectra shows that the system under study predominantly contains compounds with the molecular weight of 2166 g/mol when 0.7 L¹ equivalents are added to a porphyrin solution, which corresponds to a supramolecular dimer, in contrast to the system with an equivalent ratio of I and L¹. The molecular weights of the particles in the solution were determined based on the calculated self-diffusion coefficients (Fig. 4) that, in their turn, were found using the intensity dependences on the field gradient of these signals (Fig. S1). This method was described in [37].

4.2. Investigation of the behavior of Co-porphyrin arrays in micellar surfactant solutions.

Sulfonated porphyrins in aqueous (buffer) solutions containing molecules of cationic surfactants (S) can be found in three different forms – free monomers, surfactant-porphyrin associates and micelled porphyrins [38–42]. Our studies have shown that Co(III)-porphyrins with different ligands in buffer solutions containing molecules of cetyltrimethylammoniumbromide (CTAB) and cetylpyridinium chloride (CPC) behave in the same way [34,35,43]. Depending on the porphyrinate and surfactant concentration, different mono- and diaxial Co-

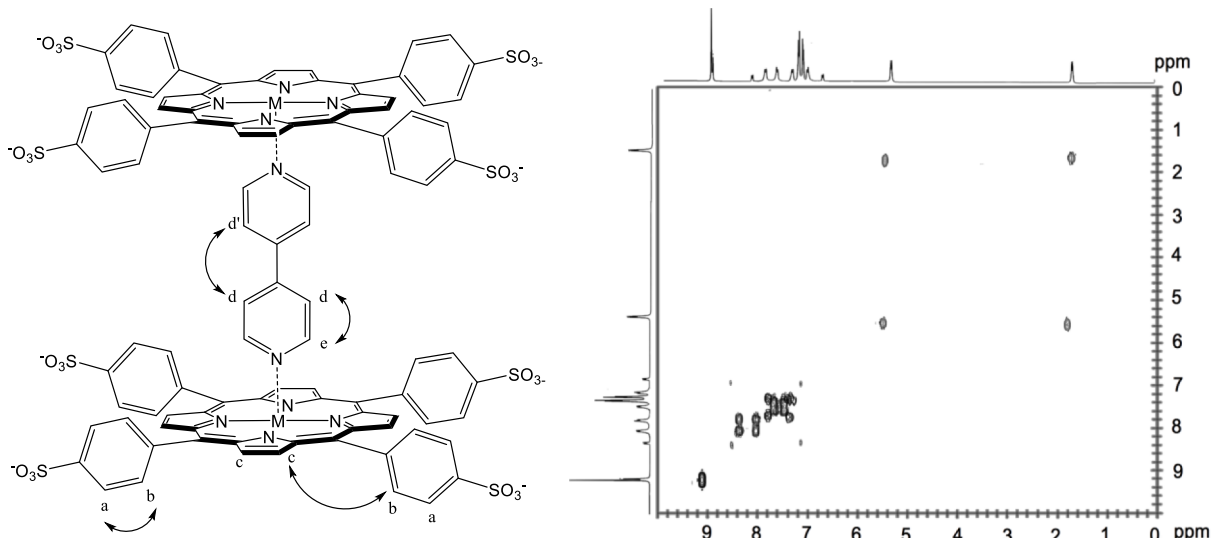


Fig. 3. Structure of the supramolecular dimer and ^1H - ^1H COSY spectrum of I-L¹-I.

Table 2
 ^1H NMR-spectra of I and its complexes with L¹.

Proton signals	L	I	I-L-I	I-L	L-I-L
H ^b (I)	-	8H, s, 9.14	16H, s 9.10	8H, s 9.12	8H, s 9.12
H ^c (I)	-	8H, d, 8.31	16H, d 7.86	8H, d 8.18	8H, d 8.11
H ^m (I)	-	8H, d, 8.12	16H, d 7.71	8H, d 7.92	8H, d 7.96
H ^c (L)	4H, d, 8.504H, d,	-	4 d 1.78	2H, d 8.49	4H, d 8.52
H ^m (L)	7.67	-	4 d 5.85	2H, d 8.49 d 2.28 2H, d 7.62 2H, d 6.40	4H, d 2.22 4H, d 7.65 4H, d 6.49

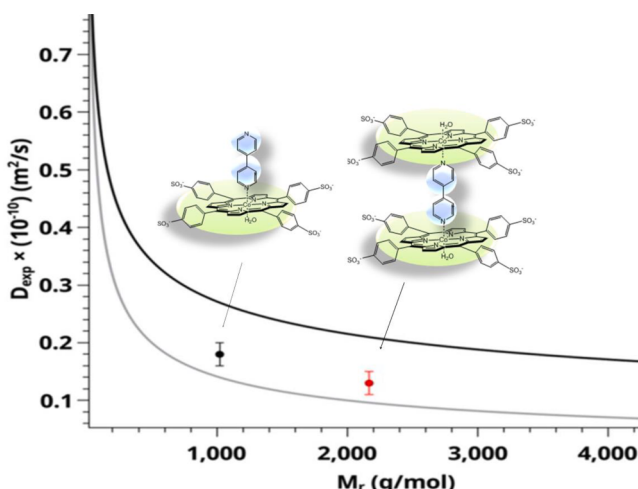


Fig. 4. Graphical analysis of the experimental values of self-diffusion coefficients (SDC) for the I-L and I-L-I complexes using signals of D₂O as a reference.

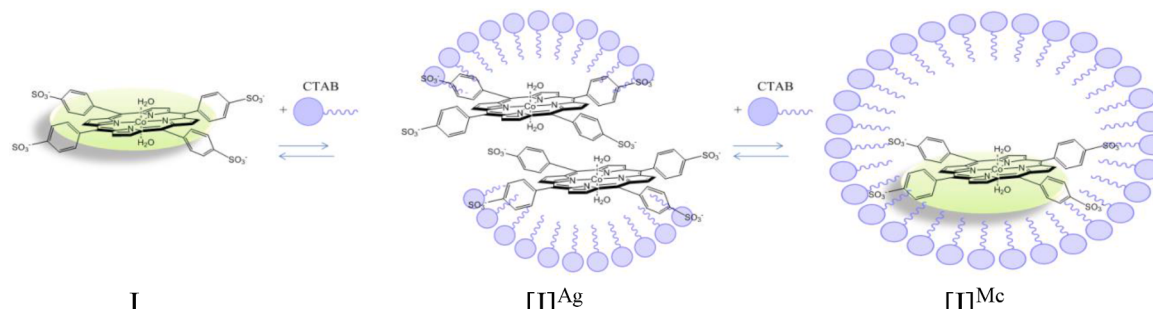
porphyrin complexes form premicellar aggregates - [CoP(L)₂]^{Ag} - or micellated porphyrinate [CoP(L)₂]^{Mc} (Scheme 2) [34,35,43]. A micellated porphyrinate is a porphyrinate located in the micelles of cationic surfactants that are formed in a solution when the critical micellar concentration is achieved [35,43].

A similar picture is observed in the porphyrin dimer. Spectrophotometric titration of the porphyrin dimer (I-L¹-I) solutions of CTAB and MTAB (Fig. 5) with small additions of surfactants causes a decrease in the electron absorption intensity, which corresponds to the formation of an [I-L¹-I]^{Ag} associate. After passing through the minimum, with a further increase in the concentration, the intensity of the absorption bands in the corresponding UV-Vis spectra begins to grow (Fig. 5), which indicates the destruction of the associates and the appearance of micellar porphyrin dimers [I-L¹-I]^{Mc}. The data of spectrophotometric CTAB-titration of the other products of interaction of I with L¹ are shown in Fig. S2.

The bigger the porphyrin compound (due to side substituents, axial coordination and dimerization), the higher the surfactant concentration is required both for the formation of the corresponding [MP]^{Ag} surfactant associates and for the formation of micellar solutions (Fig. 6). In the range of CoP < CoP(L¹) < CoP(L¹)₂ < I-L¹-I, the cmc increases from $1.2 \times 10^{-3}\text{M}$ to $2.9 \times 10^{-3}\text{M}$. It means that micellated supramolecular dimers are larger molecular systems than micellated porphyrin monomers. For example, the micellar shell of CoP, according to the spectrophotometric titration data, consists of 80 CTAB molecules, whereas the micellar shell of the porphyrin dimer includes 180 CTAB molecules. The larger micelle sizes in case of porphyrin dimers are also confirmed by dynamic light scattering data (Fig. S3). The shorter alkyl chain (by two -CH₂- groups) in the surfactant increases the CMC (critical micelle concentration). The number of surfactant molecules in the micelles immobilized by porphyrins increases with a decrease in the number of methyl groups (Fig. 6).

Using the method of dynamic light scattering we roughly estimated their hydrodynamic radii. The data obtained by spectrophotometric titration and dynamic light scattering are in good agreement. The dynamic radius of the micelles themselves is in the range from 6 to 8 nm for I and I-L¹-L, respectively (Fig. S3). As depicted in the Cryo-TEM image of 0.09 M CTAB micelles in the presence I-L-I (Fig. S4), micelle-porphyrin aggregates are slightly elongated, and characterized with a small axial ratio of ~2.

An analysis of the ^1H NMR spectra (Fig. S5 and Table 3) shows that the biggest changes in the CTAB proton signal positions when monomer molecule I is placed into a CTAB micelle are observed in the region of β -



Scheme 2.

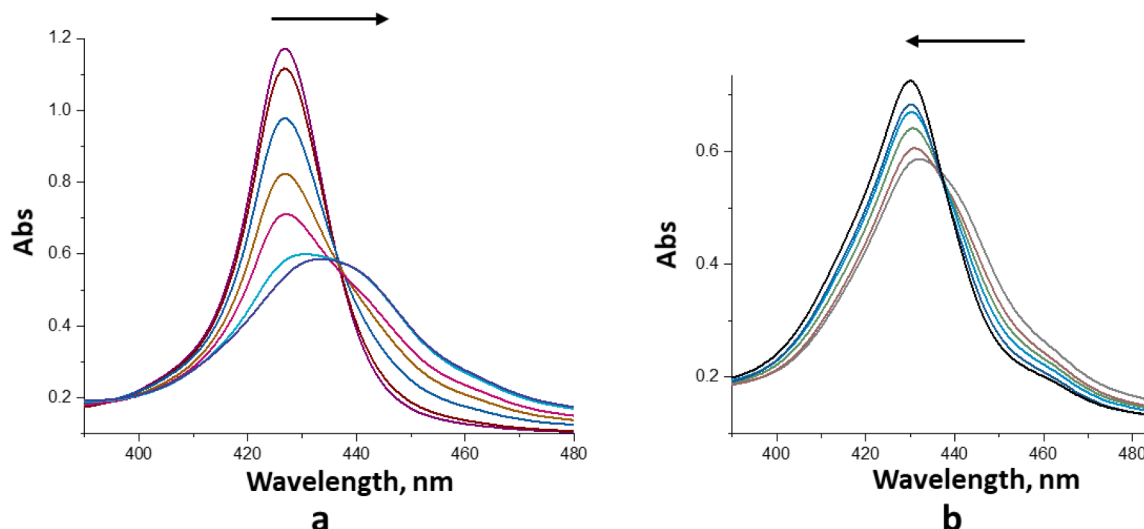


Fig. 5. UV-Vis spectra (Soret band region) of the sandwich $(\text{H}_2\text{O})\text{Co}(\text{III})\text{P-L-Co}(\text{III})\text{P}(\text{H}_2\text{O})$ complex during CTAB titration (a-b): (a) the stage of aggregate formation ($C_{\text{CTAB}} = 0\text{--}7.8 \times 10^{-4}\text{M}$), (b) the stage of micellated dimer formation ($C_{\text{CTAB}} = 7.8 \times 10^{-4}\text{--}6.4 \times 10^{-3}\text{M}$).

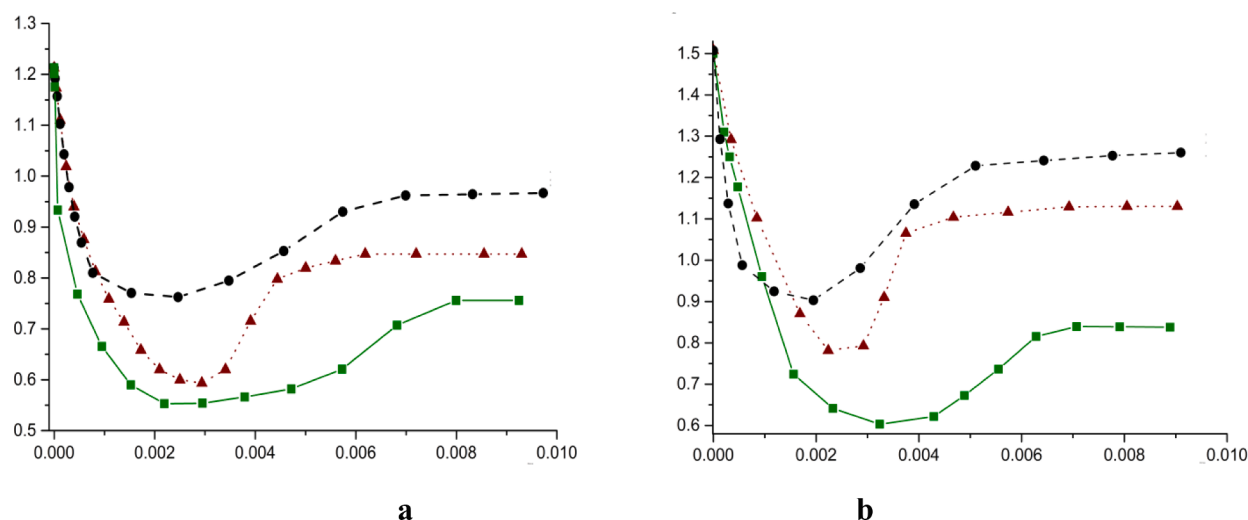


Fig. 6. $\text{L}^1\text{-I-L}^1$ (1), I-L^1 (2), $\text{I-L}^1\text{-I}$ (3) titration curves for MTAB (a) and CTAB (b) in the buffer solution (pH 7.4) at 25 °C.

and γ -protons, which indicates that the porphyrin molecule is located in the vicinity of these protons. The formation of a micellated supramolecular dimer is accompanied by changes in the CTAB proton signal positions both in β - and γ , on the one hand, and γ - and ω , on the other hand, which can be associated with deeper permeation of this compound through the CTAB micelle and simultaneous growth in its size.

We had earlier conducted a one-dimensional selective nuclear Overhauser effect experiment in order to identify the features of the CO-porphyrin interaction with the micellar CTAB solution [34]. Nuclear Overhauser effect spectroscopy is quite useful not only for studying structural characteristics of organic compounds [44–46], but also for investigating their interaction with CTAB micelles [44,45,47]. In this

Table 3

¹H NMR spectra of the CTAB micelle (CTAB -Mc), micellized monomer porphyrin I (CTAB [I]^{Mc}) and micellized supramolecular porphyrin dimer (CTAB [I-L¹-I]^{Mc}) in D₂O.

	CTAB ^{Mc}	CTAB[I] ^{Mc}	CTAB[I-L ¹ -I] ^{Mc}
CH ₃ - C	3.10(s)(12H)	3.13(s)(12H)	3.11 (s)(12H)
α (-CH ₂)	1.72(t)(2H)	1.72(br.s)(2H)	1.72(s)(2H)
β (-CH ₂)	1.32 (d)(2H)	1.32(4H)	1.32 (br.s)(4H)
γ (-CH ₂)	1.25 (d)(2H)		
δ (-CH ₂) ₁₂	1.23 (s)(24H)	1.23 (br.s)(24H)	1.16 (br.s)(24H)
ω (-CH ₃)	0.81 (t)(3H)	0.81(br.s)(3H)	0.72 (br.s)(3H)

work, we prepared a selective 1D NOESY spectrum of the porphyrin dimer under study and CTAB micelles in D₂O. To characterize the porphyrin – CTAB interaction, we applied a selective pulse tuned to the resonance frequency of pyrrole (Fig. 7 a, c) and phenyl (Fig. 7 b, d) protons in the porphyrin molecule. Selective excitation was carried out at the frequency corresponding to phenyl and pyrrole protons of the compound under study. Negative NOE signals were observed in the low-frequency part of the spectrum corresponding to the protons of the head group and aliphatic tail of the CTAB molecule. And their presence indicates that the CTAB are spatially close to the porphyrin molecule. To illustrate the contact probability and get a more detailed picture of the CTAB molecule interaction with the porphyrin, we applied the formula used to determine the cross-relaxation rates in a similar way as it had been done in work[48] for MASNOESY:

$$\sigma_{IS} = \frac{A_{IS}(t_m)}{t_m \cdot A_H(t_m)}$$

where A_{II} is the ¹D NOESY intensity of the exposed proton signal, A_{IS} is the intensity of the observed ¹D NOESY signal, τ is the time of mixing. The calculated rates are shown by bars in the CTAB molecule coordinates.

As Figure S6 shows, there is a certain ensemble-averaged picture of porphyrin interaction with CTAB molecules. In the [I]^{Mc} system, irradiation of both the pyrrole (9.06 ppm) and phenyl (8.19 ppm) fragments leads to similar distribution with the localization maximum in the γ-position of the CTAB coordinates. The structural features of the porphyrin molecules make α-localization unlikely, which is why the NOESY spectra do not show the corresponding signal. The porphyrin molecule enters micelles and localizes around the γ-segment of the CTAB molecules. The fact that there are no signals corresponding to the contact with the ω-segment in case of pyrrole fragment irradiation and their presence on the spectra in case of phenol fragment exposure indicates that the porphyrin molecule occupies a specific position inside the micelles. At the same time, a small number of CTAB molecules can be localized near the micelle surface, as indicated by the N(CH₃)₃ signals. Such molecules enter micelles only partially, like an “anchor”. The spectra of the [I-L¹-I]^{Mc} system contain both the signals of the porphyrinate fragment contacts with the γ segment and those with the δ and ω segments, which confirms again deeper permeation of the dimer through the CTAB micelle shown in Fig. S6.

4.3. Co(III)/Co(II) red-ox processes in the composition of the Co(III)P in micellar surfactant solutions

The distinguishing feature of localization of sulfonated Co(III)-porphyrinates in anionic surfactant micelles is that the hydrophobic

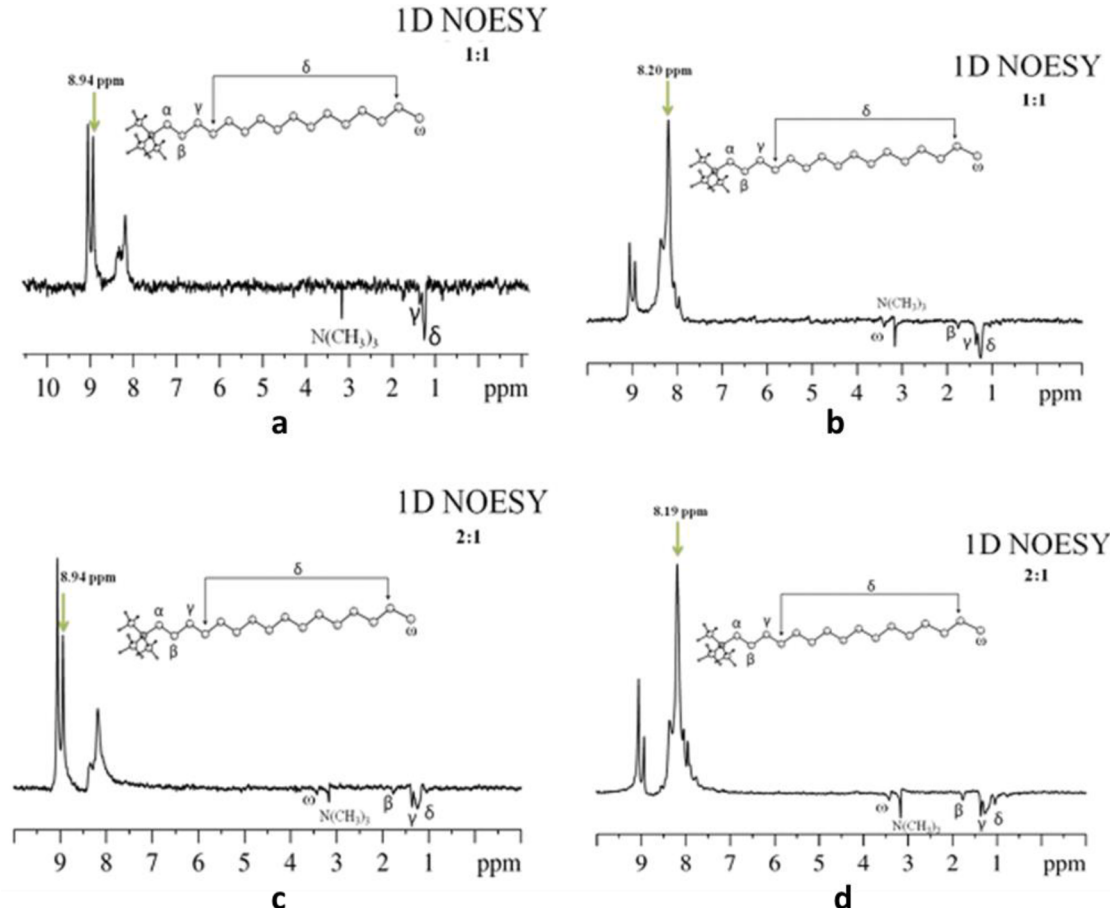


Fig. 7. 1D NOESY spectra of micellized monomer porphyrin I in the CTAB micelle (a-b) and micellized supramolecular porphyrin dimer I-L¹-I in the CTAB micelle (c-d).

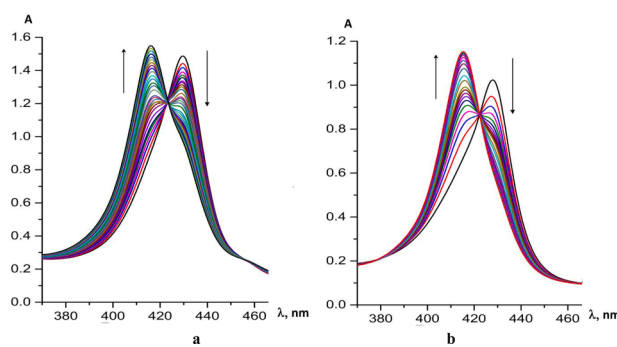


Fig. 8. Co(III) reduction to Co(II) in the micellized porphyrin dimer ($I-L^1-I$) in the CTAB micelle [the phosphate buffer pH is 7.4, the temperature is 25 °C (a), and 40 °C (b) the time is 1 day].

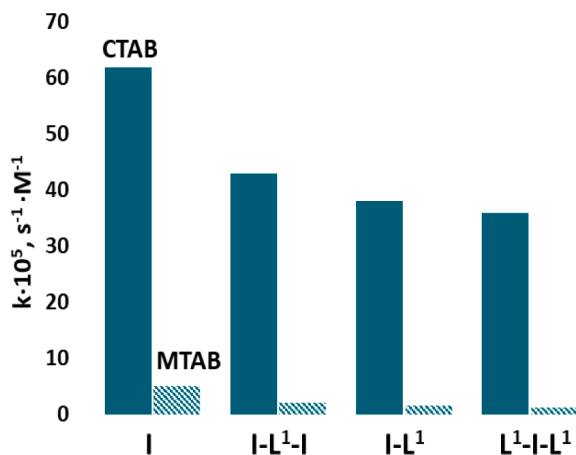


Fig. 9. Rates of reduction of $[Co(III)P(H_2O_2)]^{Mc}$, $[Co(III)P(L^1)(H_2O)]^{Mc}$, $[Co(III)P(L^1)_2]^{Mc}$ and $[Co(III)P-(L^1)-Co(III)P]$ to $[Co(II)P]^{Mc}$ (the phosphate buffer pH is 7.4, the temperature is 40 °C, the time is 6 h ($k \times 10^5, s^{-1} M^{-1}$).

medium, into which the Co(II) porphyrinate is placed, triggers Co(III) reduction to Co(II), which leads to separation of the axial ligands and in case of supramolecular dimers – to their dissociation. This process (Co (III/II) reduction) takes a certain amount of time and depends on a variety of factors – buffer and surfactant nature and temperature – and is mainly observed in porphyrinate sulfoderivatives [34,35]. As our studies have shown, the rate of Co(III)/Co(II) reduction also depends on the nature of the axial ligands on the Co(III) porphyrinate (Figs. 8 and 9 and Fig. S7, 8).

Thus, supramolecular anionic CoP-L-CoP porphyrin dimers, like monomer CoP ones, are localized in spherical surfactant micelles in micellar CTAB and MTAB solutions, but in contrast to monomer ones that are found in the palisade layer of the micelle, get deeper into the micelle. The hydrophobic environment of the porphyrinates inside the micelle causes reduction of the central Co(III) cation to Co(II) in the macrocycle coordination center, which is accompanied by separation of the axial ligands and dissociation of the supramolecular porphyrin complexes. The reduction rate can be controlled by using surfactants of different nature and concentration. It means that localization of supramolecular porphyrin complexes in micelles of a certain structure causes their prolonged destruction over the preset time.

5. Conclusion

One of the findings of the work was that self-assembly processes of hydrophilic sulfo-derivatives of Co(III)porphyrins with bidentate ligands in buffer media differ from similar processes in organic media. In organic aprotic media, supramolecular dimers based on bidentate

ligands are mostly formed by Zn(II)P, with triethylenediamine being the best complexing agent for porphyrin dimers, whereas in aqueous media, supramolecular porphyrin dimers are only formed by Co(III)porphyrins with bipyridyl. The medium pH value (within the interval of 4.0–9.0) does not produce a significant effect on the Co(III)-porphyrin properties. Formation of supramolecular Co-porphyrin dimers with bipyridyl in buffer media was studied spectrophotometrically and confirmed by the 1D and 2D 1H NMR-spectroscopy. A study was conducted of the localization processes of the prepared porphyrinate complexes and porphyrin dimers in spherical CTAB and MTAB micelles (cationic surfactants with different lengths of the alkyl tail). The differences between the localization of the monomer porphyrins and supramolecular dimers in micelles were analyzed. It was established that the depth of localization was found to be higher in the latter case. It was shown that the rate of Co (III) micellar reduction to Co(II), typical of sulfo-derivatives of Co(III) porphyrins, was lower in the dimer than in the bis-aquaporphyrinate, but higher than in its mono- and diaxial complexes with bipyridyl. The rate of Co(III) reduction to Co(II) leading to dimer (oligomer) dissociation also depends on temperature, surfactant nature and concentration. Localized deep into micelle, the macrocycle finds itself in a hydrophobic nonpolar environment. The absence of an excess of electron-donor molecules in the immediate vicinity of the metal cation contributes to the elimination of the axial ligand. The fact that in a surfactant with a large number of methylene fragments ($-CH_2-$) (CTAB) the rate of reduction of the macrocycle metal cation is higher compared to a surfactant with a smaller number of methylene fragments (MTAB), indicates that in the first case the degree of isolation of the coordination center macrocycle from unbound substrate molecules (due to spatial restrictions) is higher. This promotes faster reduction of Co(III) to Co(II) in CTAB. With an increase in temperature, the reduction of the metal cation proceeds faster. Increasing the surfactant concentration also promotes the process of metal cation reduction. The results obtained indicate the possibility of creating of supramolecular porphyrin-based assembles with the preprogrammed lifetime (from several hours to several days) and could be used as the means in the designing of biomimetic systems with effective binding affinities to heterocycles, DNA base pairs and RNA.

Declaration of Competing Interest

The authors declare that they have no known competing financial interests or personal relationships that could have appeared to influence the work reported in this paper.

Acknowledgements

This research was supported by the Russian Science Foundation (project №22-23-00018), and performed with the use of equipment of the Shared Facility Center, the Upper Volga Regional Center of Physicochemical Studies.

Appendix A. Supplementary data

Supplementary data to this article can be found online at <https://doi.org/10.1016/j.ica.2022.120972>.

References

- [1] J.L. Steed, J.W.; Atwood, Supramolecular Chemistry, 2nd ed., 2009.
- [2] I.S. Antipin, M.V. Alfimov, V.V. Arslanov, V.A. Burilov, S.Z. Vatsadze, Y. Z. Voloshin, K.P. Volcho, V.V. Gorbatchuk, Y.G. Gorbunova, S.P. Gromov, S. V. Dudkin, S.Y. Zaitsev, L.Y. Zakharchova, M.A. Ziganshin, A.V. Zolotukhina, M. A. Kalinina, E.A. Karakhanov, R.R. Kashapov, O.I. Koifman, A.I. Konovalov, V. S. Korenev, A.L. Maksimov, N.Z. Mamardashvili, G.M. Mamardashvili, A. G. Martynov, A.R. Mustafina, R.I. Nugmanov, A.S. Ovsyannikov, P.L. Padnya, A. S. Potapov, S.L. Selektor, M.N. Sokolov, S.E. Solovieva, I.I. Stoikov, P.A. Stuzhin, E. V. Suslov, E.N. Ushakov, V.P. Fedin, S.V. Fedorenko, O.A. Fedorova, Y.V. Fedorov, S.N. Chvalun, A.Y. Tsividze, S.N. Shtykov, D.N. Shurpik, M.A. Shcherbina, L.

- S. Yakimova, Functional supramolecular systems: Design and applications, Russ. Chem. Rev. 90 (8) (2021) 895–1107.
- [3] Y. Zhong, J. Wang, Y. Tian, Binary ionic porphyrin self-assembly: Structures, and electronic and light-harvesting properties, MRS Bull. 44 (2019) 183–188, <https://doi.org/10.1557/mrs.2019.40>.
 - [4] S. Kundu, A. Patra, Nanoscale strategies for light harvesting, Chem. Rev. 117 (2017) 712–757, <https://doi.org/10.1021/acs.chemrev.6b00036>.
 - [5] L. Zhu, Y. Sun, Q. Wang, S. Wu, Progress in binding affinities of metal porphyrins to heterocycles and DNA, Chin. J. Org. Chem. 29 (2009) 1700–1707.
 - [6] J.K. Sprafke, D.V. Kondratuk, M. Wykes, A.L. Thompson, M. Hoffmann, R. Drevinskas, W.-H. Chen, C.K. Yong, J. Kärnbratt, J.E. Bullock, M. Malfois, M. R. Wasielewski, B. Albinsson, L.M. Herz, D. Zigmantas, D. Beljonne, H.L. Anderson, Belt-shaped π -systems: relating geometry to electronic structure in a six-porphyrin nanoring, J. Am. Chem. Soc. 133 (2011) 17262–17273, <https://doi.org/10.1021/ja2045919>.
 - [7] B. Brizet, A. Eggenspiller, C.P. Gros, J.-M. Barbe, C. Goze, F. Denat, P.D. Harvey, B. B-diporphyrinbenzylxyloxy-BODIPY dyes: synthesis and antenna effect, J. Org. Chem. 77 (2012) 3646–3650, <https://doi.org/10.1021/jo3000833>.
 - [8] R.; Eds.; Kadish, K.M.; Smith, K.M.; Guillard, The Porphyrin Handbook, in: New York, NY, 2000; pp. 347–368.
 - [9] H.E. Toma, T. Araki, Supramolecular assemblies of ruthenium complexes and porphyrins, Coord. Chem. Rev. 196 (2000) 307–329. 10.1016/S0010-8545(99)0041-7.
 - [10] J. Wojaczynski, L. Latos-Grazyński, Poly- and oligometalloporphyrins associated through coordination, Coord. Chem. Rev. 204 (2000) 113–171, [https://doi.org/10.1016/S0010-8545\(99\)00207-6](https://doi.org/10.1016/S0010-8545(99)00207-6).
 - [11] A. Divedi, Y. Pareek, M. Ravikanth, Sn IV porphyrin scaffolds for axially bonded multiporphyrin arrays: synthesis and structure elucidation by NMR studies, Chem. Eur. J. 20 (2014) 4481–4490, <https://doi.org/10.1002/chem.201304344>.
 - [12] Y. Pareek, V. Lakshmi, M. Ravikanth, Axially bonded pentads constructed on the Sn (IV) porphyrin scaffold, Dalton Trans. 43 (2014) 6870–6879, <https://doi.org/10.1039/C3DT53619J>.
 - [13] V.S. Shetti, M. Ravikanth, Supramolecular tetrads containing Sn(IV) porphyrin, Ru (II) porphyrin, and expanded porphyrins assembled using complementary metal–ligand interactions, Inorg. Chem. 50 (2011) 1713–1722, <https://doi.org/10.1021/ic102168f>.
 - [14] I.A. Khodov, M.Y. Nikiforov, G.A. Alper, G.M. Mamardashvili, N.Z. Mamardashvili, O.I. Koifman, Synthesis and spectroscopic characterization of Ru(II) and Sn(IV)-porphyrins supramolecular complexes, J. Mol. Struct. 1081 (2015) 426–430, <https://doi.org/10.1016/j.molstruc.2014.10.070>.
 - [15] I.A. Khodov, G.A. Alper, G.M. Mamardashvili, N.Z. Mamardashvili, Hybrid multi-porphyrin supramolecular assemblies: synthesis and structure elucidation by 2D DOSY NMR studies, J. Mol. Struct. 1099 (2015) 174–180, <https://doi.org/10.1016/j.molstruc.2015.06.062>.
 - [16] C.A. Hunter, H.L. Anderson, What is cooperativity? Angew. Chem. Int. Ed. 48 (2009) 7488–7499, <https://doi.org/10.1002/anie.200902490>.
 - [17] A. Camara-Campos, C.A. Hunter, S. Tomas, Cooperativity in the self-assembly of porphyrin ladders, PNAS 103 (2006) 3034–3038, <https://doi.org/10.1073/pnas.0508071103>.
 - [18] G.M. Mamardashvili, N.Z. Mamardashvili, O.I. Koifman, Complexation of zinc octaalkylporphyrin with mono-, di-, and triethylenediamines in toluene, Russ. J. Inorg. Chem. 52 (2007) 1215–1219, <https://doi.org/10.1134/S0036023607080104>.
 - [19] N. Tran Nguyen, G.M. Mamardashvili, O.M. Kulikova, I.G. Scheblykin, N. Z. Mamardashvili, W. Dehaen, Binding ability of first and second generation/ carbazolylphenyl dendrimers with Zn(II) tetraphenylporphyrin core towards small heterocyclic substrates, RSC Adv. 4 (2014) 19703–19709, <https://doi.org/10.1039/C3RA45660A>.
 - [20] G.M. Mamardashvili, O.M. Kulikova, O.V. Maltseva, O.I. Koifman, N. Z. Mamardashvili, One and two point binding of organic bases molecules by meso-nitro substituted Sn-octaethylporphyrins, J. Porphyr. Phthalocyanines. (2014), <https://doi.org/10.1142/S1088424614500916>.
 - [21] G.M. Mamardashvili, O.M. Kulikova, N.Z. Mamardashvili, O.I. Koifman, The effect of the structure of aliphatic diamines on their interaction with zinc porphyrinates, Russ. J. Coord. Chem. 34 (2008) 427–433, <https://doi.org/10.1134/S1070328408060067>.
 - [22] N.T. Nguyen, G. Mamardashvili, M. Gruzdev, N. Mamardashvili, W. Dehaen, Binding ability of Zn-tetraarylporphyrins with two, four and eight 4-(4-(3,6-bis(t-butyl)carbazol-9-ylphenyl)-1,2,3-triazole end groups towards N-containing substrates of different nature, Supramol. Chem. 25 (2013) 180–188, <https://doi.org/10.1080/10610278.2012.741687>.
 - [23] N.S. Lebedeva, Y.A. Gubarev, N.Z. Mamardashvili, G.M. Mamardashvili, O. I. Koifman, Thermodynamic aspects of interaction zinc(II)tetraphenylporphyrin with bidentate ligands in dilute solutions, J. Incl. Phenom. Macrocycl. Chem. 84 (2016) 71–77, <https://doi.org/10.1007/s10847-015-0584-x>.
 - [24] Y. Zhang, H. Wang, R. Yang, Colorimetric and fluorescent sensing of SCN⁻ based on meso-tetraphenylporphyrin/meso-tetraphenylporphyrin cobalt(II) system, Sensors 7 (2007) 410–419, <https://doi.org/10.3390/s7030410>.
 - [25] L. Meites, Introduction to Chemical Equilibrium and Kinetics, Pergamon, Oxford, 1981.
 - [26] S. Durot, J. Taesch, V. Heitz, Multiporphyrinic cages: architectures and functions, Chem. Rev. 114 (2014) 8542–8578, <https://doi.org/10.1021/cr400673y>.
 - [27] K.M.G. Sergeev G.B., Romanov V.V., Experimental Methods of Chemical Kinetics, Vysshaya Shkola, Moscow, 1980.
 - [28] J. Stonehouse, P. Adell, J. Keeler, A.J. Shaka, Ultrahigh-quality NOE spectra, J. Am. Chem. Soc. 116 (1994) 6037–6038, <https://doi.org/10.1021/ja00092a092>.
 - [29] K. Stott, J. Stonehouse, J. Keeler, T.-L. Hwang, A.J. Shaka, Excitation sculpting in high-resolution nuclear magnetic resonance spectroscopy: application to selective NOE experiments, J. Am. Chem. Soc. 117 (1995) 4199–4200, <https://doi.org/10.1021/ja00119a048>.
 - [30] I.A. Khodov, M.Y. Nikiforov, G.A. Alper, D.S. Blokhin, S.V. Efimov, V.V. Klochkov, N. Georgi, Spatial structure of felodipine dissolved in DMSO by 1D NOE and 2D NOESY NMR spectroscopy, J. Mol. Struct. 1035 (2013) 358–362, <https://doi.org/10.1016/j.molstruc.2012.11.040>.
 - [31] D.H. Wu, A. Chen, C.S. Johnson, An Improved Diffusion-Ordered Spectroscopy Experiment Incorporating Bipolar-Gradient Pulses, J. magn. reson., Ser. A. (1995). 10.1006/jmra.1995.1176.
 - [32] K.E. Cano, M.J. Thrippleton, J. Keeler, A.J. Shaka, Cascaded z-filters for efficient single-scan suppression of zero-quantum coherence, J. Magn. Reson. (2004), <https://doi.org/10.1016/j.jmr.2003.12.017>.
 - [33] E.Y. Kaigorodova, G.M. Mamardashvili, N.Z. Mamardashvili, Axial coordination of pyridine- and imidazole-based drug molecules to Co(III)-tetra(4-carboxyphenyl) porphyrin, Russ. J. Inorg. Chem. 63 (2018) 1192–1198, <https://doi.org/10.1134/S0036023618090061>.
 - [34] G.M. Mamardashvili, E.Y. Kaigorodova, I.A. Khodov, I. Scheblykin, N. Z. Mamardashvili, O.I. Koifman, Micelles encapsulated Co(III)-tetra(4-sulfophenyl) porphyrin in aqueous CTAB solutions: Micelle formation, imidazole binding and redox Co(III)/Co(II) processes, J. Mol. Liq. 293 (2019), 111471, <https://doi.org/10.1016/j.molliq.2019.111471>.
 - [35] G. Mamardashvili, E. Kaigorodova, O. Dmitrieva, O. Koifman, N. Mamardashvili, Molecular recognition of imidazole derivatives by Co(III)-porphyrins in phosphate buffer (pH = 7.4) and cetylpyridinium chloride containing solutions, Molecules 26 (2021) 868, <https://doi.org/10.3390/molecules26040868>.
 - [36] L. Alderighi, P. Gans, A. Ienco, D. Peters, A. Sabatini, A. Vacca, Hyperquad simulation and speciation (HySS): a utility program for the investigation of equilibria involving soluble and partially soluble species, Coord. Chem. Rev. 184 (1999) 311–318, [https://doi.org/10.1016/S0010-8545\(98\)00260-4](https://doi.org/10.1016/S0010-8545(98)00260-4).
 - [37] G.M. Mamardashvili, D.A. Lazovskiy, I.A. Khodov, A.E. Efimov, N. Z. Mamardashvili, New polyporphyrin arrays with controlled fluorescence obtained by diaxial Sn(IV)-porphyrin phenolates chelation with Cu²⁺ cation, Polymers 13 (2021) 829, <https://doi.org/10.3390/polym13050829>.
 - [38] I. Giuroski, J. Furrer, M. Vermathen, Probing the interactions of porphyrins with macromolecules using NMR spectroscopy techniques, Molecules 26 (2021) 1942, <https://doi.org/10.3390/molecules26071942>.
 - [39] S.C.M. Gandini, V.E. Yushmanov, I.E. Borisovitch, M. Tabak, Interaction of the tetra(4-sulfonatophenyl)porphyrin with ionic surfactants: aggregation and location in micelles, Langmuir 15 (1999) 6233–6243, <https://doi.org/10.1021/la990108w>.
 - [40] N.C. Maiti, S. Mazumdar, N. Periasamy, J- and H-aggregates of porphyrin–surfactant complexes: Time-resolved fluorescence and other spectroscopic studies †, J. Phys. Chem. 102 (1998) 1528–1538, <https://doi.org/10.1021/jp9723372>.
 - [41] S.C.M. Gandini, V.E. Yushmanov, M. Tabak, Interaction of Fe(III)- and Zn(II)-tetra(4-sulfonatophenyl) porphyrins with ionic and nonionic surfactants: aggregation and binding, J. Inorg. Biochem. 85 (2001) 263–277, [https://doi.org/10.1016/S0162-0134\(01\)00211-2](https://doi.org/10.1016/S0162-0134(01)00211-2).
 - [42] N.C. Maiti, S. Mazumdar, N. Periasamy, Dynamics of porphyrin molecules in micelles: picosecond time-resolved fluorescence anisotropy studies, J. Phys. Chem. 99 (1995) 10708–10715, <https://doi.org/10.1021/j100027a006>.
 - [43] G.M. Mamardashvili, E.Y. Kaigorodova, O.R. Simonova, D.A. Lazovskiy, N. Z. Mamardashvili, Interaction of the Sn(IV)-tetra(4-sulfonatophenyl)porphyrin axial complexes with cetyltrimethylammonium bromide: Aggregation and location in micelles, fluorescence properties and photochemical stability, J. Mol. Liq. 318 (2020), 113988, <https://doi.org/10.1016/j.molliq.2020.113988>.
 - [44] G.M. Mamardashvili, O.V. Maltceva, D.A. Lazovskiy, I.A. Khodov, V. Borovkov, N. Z. Mamardashvili, O.I. Koifman, Medium viscosity effect on fluorescent properties of Sn(IV)-tetra(4-sulfonatophenyl)porphyrin complexes in buffer solutions, J. Mol. Liq. 277 (2019) 1047–1053, <https://doi.org/10.1016/j.molliq.2018.12.118>.
 - [45] O. Maltceva, G. Mamardashvili, I. Khodov, D. Lazovskiy, V. Khodova, M. Krest'yaninov, N. Mamardashvili, W. Dehaen, Molecular recognition of nitrogen – containing bases by Zn[5,15-bis-(2,6-dodecyloxyphenyl)]porphyrin, Supramol. Chem. 29 (5) (2017) 360–369.
 - [46] S.V. Efimov, I.A. Khodov, E.L. Ratkova, M.G. Kiselev, S. Berger, V.V. Klochkov, Detailed NOESY/T-ROESY analysis as an effective method for eliminating spin diffusion from 2D NOE spectra of small flexible molecules, J. Mol. Struct. 1104 (2016) 63–69, <https://doi.org/10.1016/j.molstruc.2015.09.036>.
 - [47] S.V. Efimov, F.K. Karataeva, A.V. Aganov, S. Berger, V.V. Klochkov, Spatial structure of cyclosporin A and insight into its flexibility, J. Mol. Struct. 1036 (2013) 298–304, <https://doi.org/10.1016/j.molstruc.2012.11.005>.
 - [48] H.A. Scheidt, D. Huster, The interaction of small molecules with phospholipid membranes studied by 1H NOESY NMR under magic-angle spinning, Acta Pharmacol. Sin. 29 (2008) 35–49, <https://doi.org/10.1111/j.1745-7254.2008.00726.x>.